Pathway of Proton Transfer in Bacterial Reaction Centers: Role of Aspartate-L213 in Proton Transfers Associated with Reduction of Quinone to Dihydroquinone†

M. L. Paddock, S. H. Rongey, P. H. McPherson, A. Juth, G. Feher, and M. Y. Okamura*

Department of Physics, 0319, University of California, San Diego, La Jolla, California 92093-0319

Received August 3, 1993; Revised Manuscript Received November 4, 1993®

ABSTRACT: The role of Asp-L213 in proton transfer to reduced quinone Q_B in the reaction center (RC) from *Rhodobacter sphaeroides* was studied by site-directed replacement of Asp with residues having different proton donor properties. Reaction centers (RCs) with Asn, Leu, Thr, and Ser at L213 had greatly reduced (~6000-fold) proton-coupled electron transfer [$k_{AB}^{(2)}$] and proton uptake rates associated with the second electron reduction of Q_B ($Q_A^-Q_B^- + 2H^+ \rightarrow Q_AQ_BH_2$) compared to native RCs. RCs containing Glu at L213 showed faster (~90-fold) electron and proton transfer rates than the other mutant RCs but were still reduced (~70-fold) compared with native RCs. These results show that $k_{AB}^{(2)}$ is larger when a carboxylic acid occupies the L213 site, consistent with the proposal that Asp-L213 is a component of a proton transfer chain. The reduced $k_{AB}^{(2)}$ observed with Glu versus Asp at L213 suggests that Asp at L213 is important for proton transfer for some other reason in addition to its proton transfer capabilities. Glu-L213 is estimated to have a higher apparent pK_a (p$K_a \geq 7$) than Asp-L213 (p$K_a \leq 4$), as indicated by the slower rate of charge recombination ($D^+Q_AQ_B^- \rightarrow DQ_AQ_B$) in the mutant RCs. The importance of the pK_a and charge of the residue at L213 for proton transfer are discussed. Based on these studies, a model for proton transfer is proposed in which Asp-L213 contributes to proton transfer in native RCs in two ways: (1) it is a component of a proton transfer chain connecting the buried Q_B molecule with the solvent and/or (2) it provides a negative charge that stabilizes a proton on or near Q_B.

The bacterial reaction center (RC)[1] from *Rhodobacter sphaeroides* is a membrane-bound bacteriochlorophyll–protein complex that performs the primary photochemistry in photosynthesis by coupling electron and proton transfer across the bacterial membrane. The bacterial RC is composed of three polypeptide subunits (L, M, and H), four bacteriochlorophylls, two bacteriopheophytins, one non-heme Fe^{2+}, and two ubiquinone (UQ_{10}) molecules [reviewed in Breton and Vermeglio (1988) and Feher *et al.* (1989)]. In the RC, light-induced electron transfer proceeds from a primary donor (a bacteriochlorophyll dimer) through a series of electron donor and acceptor molecules (a bacteriopheophytin and a quinone molecule Q_A) to a loosely bound secondary quinone Q_B. These cofactors form an **electron transfer pathway** through the photosynthetic membrane. The secondary quinone Q_B accepts two electrons from Q_A in two sequential electron transfer reactions (Figure 1). The second electron transfer is coupled with the protonation of the reduced secondary quinone. The transfer of protons to the Q_B site, which is buried within the protein matrix, has been shown to involve several amino acid residues (*e.g.*, Glu-L212 and Ser-L223) that form part of a **proton transfer pathway** from the aqueous exterior of the protein to the Q_B site (Paddock *et al.*, 1989, 1990a; Takahashi & Wraight, 1991). More recently Asp-L213 has also been implicated in the proton transfer chain (Paddock *et al.*, 1990a; Takahashi & Wraight, 1990, 1991; Rongey *et al.*, 1991).

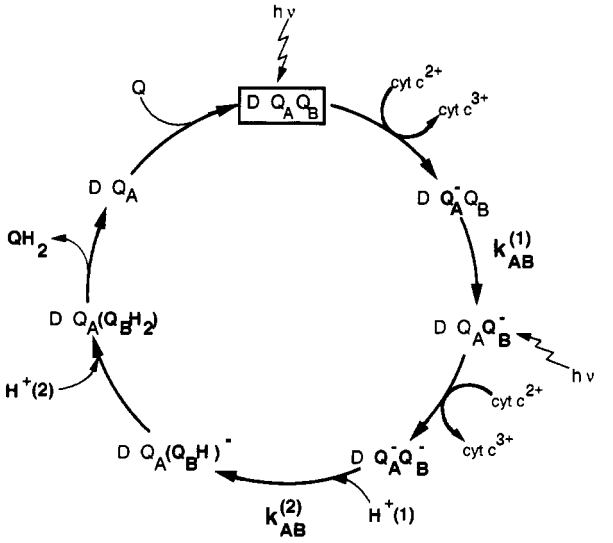

FIGURE 1: Photochemical cycle of reaction centers showing electron transfer, proton uptake, quinone exchange, and cytochrome oxidation. For each electron transfered to the quinones, one cyt molecule is oxidized. The first and second electron transfer rate constants are indicated as $k_{AB}^{(1)}$ and $k_{AB}^{(2)}$, respectively. The transfer of the second electron to Q_B involves the uptake of the first proton $H^+(1)$ (Paddock *et al.*, 1990). The transfer of a second proton $H^+(2)$ to reduced Q_B is not a prerequisite for the second electron transfer (Paddock *et al.*, 1989). The cycling rate for native RCs is $\sim 10^3$ s^{-1}.

The protonation of reduced Q_B has been investigated by proton uptake and electron transfer measurements in RCs from *Rb. sphaeroides* (Kleinfeld *et al.*, 1984, 1985; Maróti & Wraight, 1988, 1990; McPherson *et al.*, 1988). The RC

† Work supported by National Science Foundation (NSF MCB89-15631) and National Institutes of Health (NIH GM 41637 and NIH GM 13191). M.P. and P.M. were partially supported by an NIH postdoctoral training grant (5 T32 DK07233-16).

* To whom correspondence should be addressed.

® Abstract published in *Advance ACS Abstracts*, January 15, 1994.

[1] Abbreviations: D, primary donor; Q_A, primary quinone acceptor; Q_B, secondary quinone acceptor; Q, quinone molecule; QH_2, dihydroquinone; UQ_{10}, ubiquinone-50; RC, reaction center; cyt *c*, horse heart cytochrome *c*; bp, base pair; HMK, 10 mM Hepes, pH 7.5, 0.04% maltoside, and 50 mM KCl.

0006-2960/94/0433-734$04.50/0

photocycle consists of electron transfer, proton transfer, and quinone exchange steps (Figure 1). The first electron reduction of Q_B to Q_B^- [$k_{AB}^{(1)}$] is not accompanied by direct protonation of Q_B^- (Figure 1). The second electron reduction, on the other hand, is accompanied by the uptake of two protons from solution, forming the dihydroquinone Q_BH_2. The pathway of this proton transfer from solution to reduced Q_B has been investigated by studying the rates of electron and proton transfers in RCs with site-directed modifications. Replacement of Glu-L212 with Gln greatly decreased the rate of proton uptake (McPherson *et al.*, 1990) but did not affect the rate of electron transfer (Paddock *et al.*, 1989), while replacement of Ser-L223 with Ala decreased the rates of both proton uptake and electron transfer (Paddock *et al.*, 1990a).[2] These results were interpreted to indicate that the two protons required to form QH_2 (Figure 1) are taken up by separate pathways (Paddock *et al.*, 1990a). The first proton [$H^+(1)$] is taken up by a pathway involving Ser-L223 and is **coupled** to electron transfer; the second proton [$H^+(2)$] is taken up by a pathway involving Glu-L212 **following** electron transfer.

In the present work we investigated the role of Asp-L213 in proton transfers associated with the double reduction of Q_B. It was previously reported that electron and proton transfer rates were much reduced when Asp-L213 was replaced with Asn (Paddock *et al.*, 1990a; Takahashi & Wraight, 1990, 1991; Rongey *et al.*, 1991), suggesting that Asp-L213 was a component of a proton transfer chain leading to Q_B. However, there are alternate models to explain the data. To clarify the role of Asp-L213 in proton transfer, electron and proton transfer rates were measured in RCs in which Asp-L213 was replaced by the proton donor groups Ser, Thr, and Glu as well as by Asn and Leu. We measured the dependences of $k_{AB}^{(2)}$ (Figure 1) on pH and on the concentration of azide (NaN_3), a mobile protonophore that had been found to increase the rates of proton transfer in halorhodopsin (Hegemann *et al.*, 1985; Lanyi, 1986), bacteriorhodopsin (Tittor *et al.*, 1989), and bacterial RCs (Takahashi & Wraight, 1991). Charge recombination was measured as a function of pH for native and mutant RCs. The results are discussed in terms of the roles of Asp-L213 as a proton donor group and as a residue that establishes proper electrostatics near reduced Q_B. Preliminary reports of this work have been previously published (Paddock *et al.*, 1990a, 1991a; McPherson *et al.*, 1991; Rongey *et al.*, 1991; Feher *et al.*, 1992).

MATERIALS AND METHODS

Materials. Dodecyl β-D-maltoside was obtained from Calbiochem, deoxycholic acid from Sigma, and LDAO (*N*,*N*-dimethyldodecylamine N-oxide) from Fluka Chemie. Ubiquinone-50 was obtained from Sigma and was solubilized at 50 °C in either 10% deoxycholic acid (at ~1 mM quinone) or 1% LDAO (at ~0.2 mM quinone) and stored at −70 °C. Horse heart cytochrome *c* (cyt *c*, type 6, Sigma) was reduced by hydrogen gas in the presence of platinum black (Aldrich) and purified by filtration through cellulose acetate (Millipore). The pH indicator dye phenol red was obtained from Sigma. Restriction enzymes and other DNA-modifying enzymes used in the site-directed mutagenesis procedures were obtained as described in Paddock *et al.* (1989). The site-directed mutagenesis kit was obtained from Amersham. The BBL GasPak jar systems were obtained from Fisher Scientific (Tustin, CA). All other reagents were of reagent or HPLC grade.

[2] Control experiments where Glu-L212 was replaced by Asp (Paddock *et al.*, 1989) and Ser-L223 was replaced by Thr (Paddock *et al.*, 1990a) restored the rates to within 2–4-fold of the native rates.

Site-Directed Mutagenesis. The construction of the site-directed mutants was performed as described in Paddock *et al.* (1989) with a few modifications as noted. The mutagenesis was performed using the Amersham oligonucleotide-directed mutagenesis kit based upon the method developed by Nakamaye and Eckstein (1986). Oligonucleotides were synthesized to replace the native GAT codon for Asp-L213 (Williams et al., 1984): (1) 5′-GATCACGAG **AAC** ACGTTCTTCC-3′ for the Asp-L213 → Asn mutation carrying the **AAC** codon for Asn; (2) 5′-GGATCACGAG **CTG** ACGTTCTTCC-3′ for the Asp-L213 → Leu mutation carrying the **CTG** codon for Leu; (3) 5′-CCGGATCACGAG (A/T)CG ACGTTCTTCCGC-3′ for the Asp-L213 → Ser, Thr mutations carrying either the **TCG** codon for Ser or the **ACG** codon for Thr; (4) 5′-CCGGATCACGAG (G/A)AG ACGTTCTTCCGC-3′ for the Asp-L213 → Glu, Lys mutations carrying either the **GAG** codon for Glu or the **AAG** codon for Lys.

The mutations were incorporated into an M13 vehicle containing the *Pvu*II–*Sal*I fragment [490 base pairs] which contains the DNA coding for the latter two-thirds of the L subunit (Paddock *et al.*, 1990a). Mutants were identified by single-lane sequencing of phage DNA from several dozen plaques. A uniform phage culture for each replacement was obtained by reinfection into *Escherichia coli* followed by isolation of an individual plaque. The sequence of the entire insert region was determined for these uniform phage cultures. No changes other than the desired mutations were noted in the *Asp* 718–*Sal* I region. This fragment was then exchanged with the kanamycin fragment of pRKENKm (Paddock *et al.*, 1989) resulting in the expression vehicles pRKMUT with the DN(L213) (Asp-L213 → Asn), DL(L213) (Asp-L213 → Leu), DS(L213) (Asp-L213 → Ser), DT(L213) (Asp-L213 → Thr), or DE(L213) (Asp-L213 → Glu) mutation. These were transformed into *E. coli* S17-1 (Simon *et al.*, 1983) and mated into the *Rb. sphaeroides* deletion strain ΔLM1 resulting in the complemented deletion strains. These strains were grown semiaerobically to induce RC production without applying selection for photosynthetic growth as described (Paddock *et al.*, 1989).

The photosynthetic growth of the complemented deletion strains carrying the native or site-directed modified RC genes were tested as described (Rongey *et al.*, 1993). Briefly, the deletion strain complemented with native or mutant genes was restricted to anaerobic photosynthetic conditions using the BBL GasPak 100 or 150 jar systems. Control plates grown aerobically were used to determine the original viable cell density.

Reaction Center Preparation. RCs were isolated in LDAO as described (Paddock *et al.*, 1988); they contained approximately 1–1.5 quinone/RC as determined by standard methods (Kleinfeld *et al.*, 1984) and had an observed ratio of $A_{280}^{1cm}/A_{802}^{1cm} \leq 1.25$ for the DN(L213), DL(L213), and DE(L213) RCs and $A_{802}^{1cm}/A_{802}^{1cm} \leq 1.6$ for the DS(L213) and DT(L213) RCs. The RC concentration was determined (McPherson *et al.*, 1993a) by the amount of cyt *c* oxidized (measured at 550 nm) after one saturating laser flash using $\epsilon_{cytc^{2+}}^{550} - \epsilon_{cytc^{3+}}^{550} = 21.1\ mM^{-1}\ cm^{-1}$ (Van Gelder & Slater, 1962). Reconstitution of Q_B into the RCs was accomplished as follows: a 5–10-fold excess of UQ_{10} was added to the RC solution ($A_{802}^{1cm} \sim 2$) which was then dialyzed for 2 days against 0.04% dodecyl β-D-maltoside, 8 mM KCl, and either 2 mM Tris or 2 mM Ches at pH 7.5 or 9. High pH was used for the mutant RCs to destabilize the $DQ_AQ_B^-$ state to avoid the accumulation of this state in view of its long lifetime in the mutant RCs (see results). Native RCs were also prepared with 2 UQ_{10}/RC following the same procedure. The RCs

were concentrated to a final absorbance of $A_{802} \geq 50$ and stored at −70 °C.

Electron Transfer Rate Measurements. The kinetics of electron transfer were determined from absorption changes recorded on a modified Cary 14 spectrophotometer (Varian) as described by Kleinfeld *et al.* (1984). All measurements were performed with 1–3 μM RCs in 10 mM buffer(s), 0.04% dodecyl β-D-maltoside, and 50 mM KCl at 23 °C. All electron transfer rates for native, DN(L213), and DE(L213) RCs were measured in the presence and absence of excess quinone and were found to be the same. In addition, electron transfer rates for the L213 mutants were measured in the presence of equimolar amounts of ferricyanide, which was found to reduce the amount of $DQ_AQ_B^-$ present in the dark samples without altering the measured kinetic decay rates. The rate constant for the transfer of the first electron to Q_B, $k_{AB}^{(1)}$ (Figure 1), was measured by monitoring the bacteriopheophytin band shift at 750.5 nm, which is sensitive to the reduction state of the quinones Q_A and Q_B (Kleinfeld *et al.*, 1984). The measured rate constant for the double reduction of Q_B, $k_{AB}^{(2)}$ (Figure 1), was determined by measuring the decay after a second laser flash of the semiquinone absorption at 450 nm (Kleinfeld *et al.*, 1985) in the presence of 20–50 μM cytochrome *c* (cyt *c*), which reduces the donor after each flash. The charge recombination rate $D^+Q_A^- \rightarrow DQ_A$ (k_{AD}) was determined from the rate of recovery of the oxidized donor monitored at 865 nm following a saturating laser flash in RCs containing only Q_A. The charge recombination rate $D^+Q_AQ_B^- \rightarrow DQ_AQ_B$ (k_{BD}) was determined from the kinetics of the slow phase of the donor recovery (~30–90% of the amplitude) in RC samples in the presence of excess UQ_{10}. Special care was taken to avoid exposure to light in treating and measuring the small recombination rate k_{BD} in the DN(L213), DL(L213), DS(L213), DT(L213), and DE(L213) mutant RCs. The pH of the solution was adjusted by adding acid (HCl) or base (NaOH) to a mixture of buffers containing Caps, Ches, Mes, Pipes, and Tris at 2.5 mM each. The NaN_3 (azide) and NaCl concentrations were adjusted by adding to the RC solution known amounts of NaN_3 or NaCl, solubilized at 5 M in the buffer solution at the appropriate pH.

Cytochrome turnover was measured by monitoring the oxidation of cyt *c* at 550 nm [see, *e.g.*, Paddock *et al.* (1990a)] by the RCs in the presence of excess UQ_{10} and cyt *c* under continuous illumination ($I = 1$ W/cm^2). RCs were illuminated perpendicular to the monitoring beam of a Cary 14 spectrophotometer with continuous illumination from a 500-W projector through 1 in. of water and a Corning 2-64 filter. [Conditions: 0.7–1 μM RCs with excess UQ_{10} per RC in HMK buffer with 25–50 μM cyt *c*. Ferricyanide (1 μM) was added to the L213 mutant RC samples.] The rate of cyt *c* photooxidation (per RC) was determined from the change in absorbance at 550 nm normalized to the change in absorbance at 550 nm after a single saturating laser flash (representing 1 cyt *c* oxidized/RC).

Proton Uptake Measurements. Proton uptake was determined at pH 7.5 by measuring the optical absorbance change at 557 nm of the pH indicator dye phenol red following saturating laser pulses (McPherson *et al.*, 1993a). The change in absorbance was calibrated in terms of proton uptake by adding known amounts of HCl with a syringe (Hamilton 701; 10-μL capacity). Native and mutant RCs contained a 5–10-fold excess of UQ_{10} per RC to maximize the occupancy of the Q_B site (>80%). (Conditions: 1.5 μM RCs, 50 μM phenol red, 25 μM cyt *c*, 50 mM KCl, 0.04% dodecyl β-D-maltoside, pH 7.5, 23 °C.)

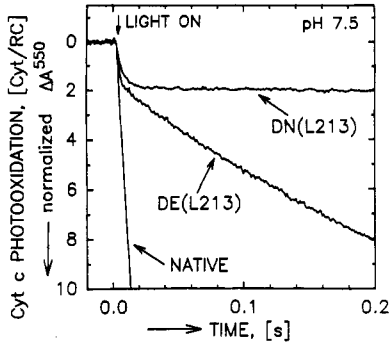

FIGURE 2: Cytochrome photooxidation in native, DN(L213) (Asp-L213 → Asn), and DE(L213) (Asp-L213 → Glu) RCs. The photooxidation of cyt *c* was monitored at 550 nm in the presence of exogenous quinone and cyt *c* under continuous illumination. (Conditions: 0.7 μM RCs, 25 μM cyt *c*, 10 mM Hepes at pH 7.5, 0.04% dodecyl β-D-maltoside or 0.025% deoxycholic acid, 1 μM ferricyanide, $I = 1$ W cm^{-2}, 23 °C.) The normalization to (cyt/RC) was determined from the absorbance change at 550 nm after a single saturating laser flash (representing 1 cyt oxidized/RC). The cyt *c* photooxidation observed in native RCs was all fast (≥7 cyt/RC) at a rate of ≥500 (cyt/RC) s^{-1}. The DN(L213) RCs show a fast oxidation ($k \geq 500$ s^{-1}) of 1.8 cyt/RC followed by a slow steady-state turnover of 0.5 (cyt/RC) s^{-1}. The DE(L213) RCs show a fast oxidation of 1.8 cyt/RC followed by a slower steady-state turnover at a rate of 38 (cyt/RC) s^{-1}.

RESULTS AND ANALYSIS

Construction and Growth of the Asp-L213 Mutants. The replacements of Asp-L213 with Asn, Leu, Ser, Thr, and Glu were constructed and transferred into the deletion strain ΔLM1 as described in Materials and Methods. The ability of the strains carrying native or mutant RC genes to grow under photosynthetic conditions was tested by comparing the number of colonies present on a plate grown under photosynthetic conditions with those on duplicate plates grown under nonselective aerobic conditions. Total numbers of bacteria used were 10^3, 10^5, and 10^7. The complemented deletion strain carrying the native *puf* operon, which includes the genes coding for the native L and M subunits, showed a comparable number of colonies on duplicate plates grown under aerobic and anaerobic (photosynthetic) conditions. The complemented deletion strains carrying any of the mutant *puf* operons showed only a small fraction ($<10^{-5}$) of colonies on the anaerobic plate compared to the aerobic plate. These photosynthetic viable colonies are attributed to revertants containing suppressor mutations that restore photosynthetic function to the RCs. Thus, the removal of Asp-L213 resulted in photosynthetically deficient strains.

Cytochrome Photooxidation. The photooxidation of cytochrome by RCs was used to measure the flow of electrons and protons through the RC photocycle (Figure 1). A reduced rate for any one step can result in a decrease in the cytochrome turnover rate. For each electron transferred to the quinones (see Figure 1), 1 cyt *c* molecule/RC (cyt/RC) is oxidized. Following the onset of illumination, cyt *c* is rapidly ($k \geq 1000$ s^{-1}) oxidized by RCs until the photocycle reaches the rate-limiting step. The subsequent rate of steady-state turnover is determined by the rate of this step.

Measurements on the native and the mutants DN(L213) (Asp-L213 → Asn) and DE(L213) (Asp-L213 → Glu) were performed in the presence of exogenous quinone and cyt *c* under continuous illumination and are shown in Figure 2 (pH 7.5). Native RCs show rapid ($k \geq 500$ s^{-1}) oxidation of ≥7 cyt/RC; the turnover is ultimately limited by the amount of exogenous quinone present in the sample. In contrast, DN(L213) RCs show a rapid oxidation ($k \geq 500$ s^{-1}) of only 1.8 cyt/RC followed by a slower steady-state turnover at a

Table 1: Comparison of Electron Transfers in Native and Mutant RCs (pH 7.5)[a]

reaction	rate constant	assay	rate, s^{-1} native[b]	DN(L213)	DE(L213)
photocycle rate[c]	k	1	>500	0.25	19
$D^+Q_A^- \rightarrow DQ_A$	k_{AD}	2	9.5	10	10
$DQ_A^-Q_B \rightarrow DQ_AQ_B^-$	$k_{AB}^{(1)}$	3	6800	600	6800
$D^+Q_AQ_B^- \rightarrow DQ_AQ_B$	k_{BD}	2	0.70	0.04	0.02
$DQ_A^-Q_B^- + H^+ \rightarrow DQ_A(Q_B^{2-}H^+)$	$k_{AB}^{(2)}$	4	1500	0.25	17

[a] RC concentrations were 0.3–3 μM. Assay 1: cyt *c* oxidation monitored at 550 nm (Paddock *et al.*, 1989) (25 μM cyt). Assay 2: donor recovery monitored at 865 nm (Kleinfeld *et al.*, 1984). Assay 3: bacteriopheophytin band shift monitored at 750.5 nm (Kleinfeld *et al.*, 1984). Assay 4: semiquinone signal monitored at 450 nm (Kleinfeld *et al.*, 1985) (50 μM cyt or 500 μM ferrocene). There was a variation of ~25% in the rates depending on the particular RC preparation and age of the sample. [b] Native represents R26 or 2.4.1 RCs; the two strains gave the same results. [c] The photocycle rate is defined as the number of complete cycles (Figure 1) turned over per second upon continuous excitation and is equal to one-half of the cytochrome turnover rate since two cyt molecules are oxidized per cycle (Figure 1).

rate of 0.5 (cyt/RC) s^{-1}, which is >1000-fold slower than in native RCs. The fast phase of 1.8 cyt/RC suggests the fast formation of the $DQ_A^-Q_B^-$ state in the 80% of the RCs that had a bound Q_B molecule (based on the fraction of RCs displaying slow charge recombination). The remaining 20% of the RCs that lack Q_B reach the DQ_A^- state with no further photochemistry. Thus 2.0 cyt/DQ_AQ_B were oxidized rapidly. Similar results were obtained in the DL(L213), DS(L213), and DT(L213) RCs (data not shown).

The DE(L213) RCs show a rapid oxidation of 1.8 cyt/RC (*i.e.*, 2.0 cyt/DQ_AQ_B) followed by a turnover rate of 38 (cyt/RC) s^{-1} (Figure 2). The cytochrome photooxidation measurements show that the $Q_A^-Q_B^-$ state is reached rapidly ($k \geq 500$ s^{-1}) in the majority of the RCs with a bound Q_B molecule. The steady-state turnover rate of 38 (cyt/RC) s^{-1}, limited by the subsequent step $k_{AB}^{(2)}$ (Figure 1), is ~80-fold faster than observed in the other L213 mutant RCs; it is, however, still at least 13-fold slower than native RCs (pH 7.5).

Forward Electron Transfer Rates. The rapid oxidation of 2.0 cyt/DQ_AQ_B in all of the mutant RCs indicates that the electron transfer rates leading to a two-electron reduction of the quinones (*i.e.*, $Q_A^-Q_B^-$) are fast. Further reactions are limited by the subsequent proton-coupled electron transfer $k_{AB}^{(2)}$ (Figure 1). To test this hypothesis, the electron transfer rates for the individual steps in the cycle were measured by monitoring transient optical absorption changes in native and mutant RCs.

(*A*) $k_{AB}^{(1)}$:$Q_A^-Q_B \rightarrow Q_AQ_B^-$. The electron transfer rate constant $k_{AB}^{(1)}$ was measured in native and mutant RCs (Table 1) by monitoring the absorbance at 750.5 nm, which is sensitive to the reduction state of the quinones (Kleinfeld *et al.*, 1984). The DN(L213), DL(L213), DS(L213), and DT(L213) mutant RCs showed a reduced rate ($k_{AB}^{(1)} \sim 500$ s^{-1}) compared to the native RCs (7000 s^{-1}). The DE(L213) RCs showed fast electron transfer ($k_{AB}^{(1)} \sim 6800$ s^{-1}) similar to that observed in native RCs (pH 7.5). A minor fraction (<20%) displayed slower kinetics attributed to those RCs starting in the $DQ_AQ_B^-$ state before the measurement which displayed $k_{AB}^{(2)}$ kinetics. These results are in agreement with the cytochrome photooxidation measurements, which showed that the RCs rapidly ($k \geq 500$ s^{-1}) reach the $Q_A^-Q_B^-$ state in all mutant RCs.

(*B*) $k_{AB}^{(2)}$:$Q_A^-Q_B^- + H^+ \rightarrow Q_AQ_B^{2-}H^+$. The rate constant $k_{AB}^{(2)}$ was measured by monitoring the decay of the semiquinone absorbance at 450 nm after two laser flashes in the presence of exogenous donors (Kleinfeld *et al.*, 1985). Figure 3 shows the absorbance changes at 450 nm for native and DN(L213) RCs (pH 7.5) in the presence of cytochrome *c*. After the first flash both native and mutant RCs form the state $Q_AQ_B^-$ as shown by the increase in absorbance at 450 nm; oxidized cytochrome *c* also absorbs at 450 nm and causes ~50% of the absorbance increase [see, *e.g.*, Kleinfeld *et al.* (1985)].

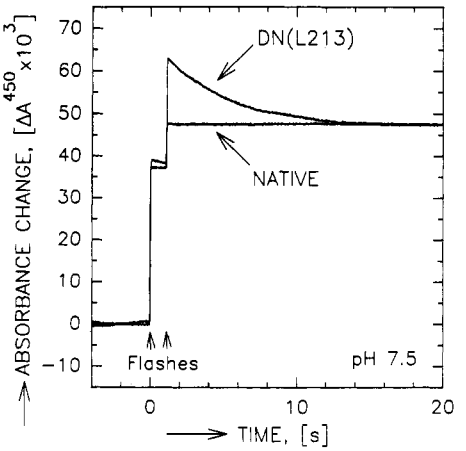

FIGURE 3: Electron transfer kinetics used to determine $k_{AB}^{(2)}$ monitored *via* the absorbance of semiquinone at 450 nm as a function of time at pH 7.5. The absorbance increased after the first flash due to the formation of $Q_AQ_B^-$ and the oxidation of one cytochrome molecule. A transient absorbance increase due to the formation of the $Q_A^-Q_B^-$ state was seen in the DN(L213) RCs after the second flash. This absorbance decayed due to the formation of the doubly reduced Q_B state at a rate $k_{AB}^{(2)} = 0.25$ s^{-1}. In native RCs the decay was too rapid (~1500 s^{-1}) to be resolved under the conditions shown. (Conditions: ~3 μM RCs, 20 μM cytochrome *c*, 1 μM ferricyanide, in HMK buffer, 23 °C.) The traces were scaled to have the same absorbance at long times (20 s) after the second flash. The slight decay observed after the first flash in the DN(L213) RCs is due to the fraction of RCs in the state $DQ_AQ_B^-$ prior to the first flash. This state is very stable in the DN(L213) RCs (see results on charge recombination). The residual absorbance seen at long times after the second flash was due mainly to the absorbance of oxidized cytochrome *c* formed upon charge separation.

After the second flash there is a transient increase in absorption due to the formation of $Q_A^-Q_B^-$. In native RCs (pH 7.5) the semiquinone absorbance decays rapidly (too fast to resolve in Figure 3 but observable on an expanded time scale), due to the fast formation of doubly reduced Q_B, with a value of $k_{AB}^{(2)} = 1500$ s^{-1} (Table 1). However, in the DN(L213) mutant RCs the semiquinone absorbance decays slowly, due to the slower formation of doubly reduced Q_B, with a value of $k_{AB}^{(2)} = 0.25$ s^{-1} (6000-fold smaller than in native RCs). Partial restoration of this rate is observed in the DE(L213) RCs (Table 1) with a value of $k_{AB}^{(2)} = 17$ s^{-1} (90-fold slower than the native rate). The values of $k_{AB}^{(2)}$ observed in the DL(L213), DS(L213), and DT(L213) RCs were essentially the same as that of the DN(L213) RCs (0.2–0.6 s^{-1}). The measured value of $k_{AB}^{(2)}$ in the mutant RCs is approximately the same as the photocycle rate determined from the cytochrome photooxidation measurements, consistent with the proton-coupled electron transfer $Q_A^-Q_B^- + H^+ \rightarrow Q_AQ_B^{2-}H^+$ being the rate-limiting step in the cycle. The lack of recovery to the preflash baseline following the second flash is due mainly to the absorbance of oxidized cyt *c* formed during the measurement.

A slight decay of the amplitude at 450 nm was observed after the first flash in the DN(L213) (Figure 3) and was more prevalent in the DE(L213) RCs (not shown). This is presumably due to the presence of a fraction of RCs in the

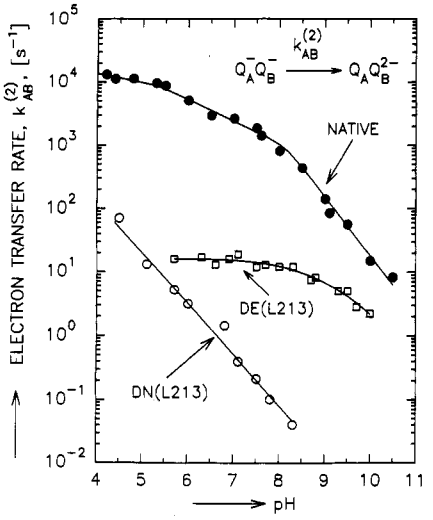

FIGURE 4: pH dependence of the electron transfer rate constant $k_{AB}^{(2)}$ determined as described in Figure 3. [Conditions: ~1–3 μM RCs; 20–500 μM ferrocene or 20 μM cytochrome *c* (for the DN(L213) RCs); 2 mM each Hepes, Caps, Ches, Mes, Pipes, and Tris; 0.04% dodecyl β-D-maltoside; 50 mM KCl; 1 μM ferricyanide, 23 °C.] The pH was adjusted by adding HCl or NaOH.

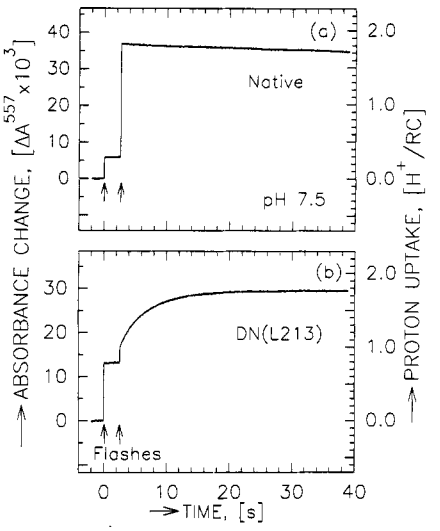

FIGURE 5: Proton uptake by (a) native and (b) DN(L213) RCs in the presence of exogenous cyt *c* after each of two saturating laser flashes at pH 7.5. A small correction (~5%) due to the absorbance changes of the RCs and cyt *c* has been subtracted. The proton uptake was calibrated by adding a known amount of HCl. The absorbance change after the first flash is a result of proton uptake by amino acid residues whose pK_a was shifted upon formation of Q_B^- (Maróti & Wraight, 1988; McPherson *et al.*, 1988). After the second laser flash, native RCs take up protons rapidly (k > 500 s^{-1}), indicating that Q_BH_2 is formed in <2 ms. The total uptake was 2.0 H^+/Q_B^{2-} after making the appropriate corrections as discussed in McPherson *et al.* (1993a). The DN(L213) RCs show slow proton uptake after the second flash (k = 0.23 s^{-1}) concomitant with the second electron transfer to Q_B (see Figure 3). The total proton uptake in the mutant was also 2.0 H^+/Q_B^{2-} after appropriate corrections. (Conditions: 1.5 μM RCs, 50 μM phenol red, 25 μM cyt *c*, 50 mM KCl, 0.04% dodecyl β-D-maltoside, pH 7.5, 23 °C.)

$DQ_AQ_B^-$ state in the dark sample. Indeed, in these samples an EPR spectrum (not shown) indicative of the native Fe^{2+}–Q_B^- spectrum was observed, consistent with the presence of the $DQ_AQ_B^-$ state in the dark. This effect becomes less prevalent below pH ~ 6. The addition of ferricyanide removed most of the dark $DQ_AQ_B^-$ state. For example, 20 μM ferricyanide reduced the amount of dark $DQ_AQ_B^-$ from ~85% to <10% in the DE(L213) RCs within 15 min at pH 10.

Since the double reduction of Q_B is coupled to proton transfer, the pH dependence of $k_{AB}^{(2)}$ (Figure 4) provides important information about the mechanism of this reaction. A logarithmic plot of the rate constant versus pH for the DN(L213)[3] RCs shows that $k_{AB}^{(2)}$ is proportional to $[H^+]^{0.85}$. In contrast, native RCs show a rate constant that is proportional to $[H^+]^{0.4}$ at pH ≤ 8 and to $[H^+]^{1.0}$ at pH ≥ 8.[4] In the DE(L213) RCs the observed rate $k_{AB}^{(2)}$ was found to be approximately pH-independent from 6 ≤ pH ≤ 9 (the RCs appeared unstable below pH ~ 6) and proportional to $[H^+]^{0.9}$ above pH ~ 9.[5] At high pH, $k_{AB}^{(2)}$ in native and DE(L213) RCs converge; at pH 9.5, $k_{AB}^{(2)}$ measured in the DE(L213) RCs was only ~5-fold slower than the native rate.

(C) Azide Effect. To test the hypothesis that the reduced $k_{AB}^{(2)}$ in the DN(L213) RCs is due to a decreased rate of proton transfer, we measured $k_{AB}^{(2)}$ in the presence of azide (NaN_3), a known protonophore (Hegemann *et al.*, 1985; Lanyi, 1986; Tittor *et al.*, 1989). For the DN(L213) RCs, the addition of NaN_3 had a maximum effect at pH 7.5 with an ~40-fold enhancement in $k_{AB}^{(2)}$ at 1 M NaN_3. Above 1 M NaN_3 the rate decreased. Control experiments with NaCl showed essentially no enhancement on the rate suggesting that N_3^- (or HN_3) is the active species. Above pH 8 or below pH 5, NaN_3 had essentially no effect on $k_{AB}^{(2)}$. Similar effects of NaN_3 and other small acids were observed in the DN(L213) mutant by Takahashi and Wraight (1991). It should be noted that the rate observed in the DN(L213) RCs in the presence of ~1 M NaN_3 was essentially the same as the $k_{AB}^{(2)}$ observed in the DE(L213) RCs without azide. No enhancement of the rate was observed in the DE(L213) RCs in the presence of azide (500 mM); in this mutant a slight (~20%) decrease was observed.

Proton Uptake. The most direct test for altered proton transfer in the DN(L213) RCs involved the measurement of the light-induced rate of proton uptake from solution (pH 7.5) using a pH-sensitive dye (phenol red) following the formation of the reduced quinones (Figure 5).

Following one flash the state $DQ_AQ_B^-$ is formed, which results in an absorbance increase (Figure 5) due to proton uptake from residues whose pK_as are shifted by the electrostatic interaction with Q_B^- (Maróti & Wraight, 1988; McPherson *et al.*, 1988). The rate of proton uptake was concomitant with $k_{AB}^{(1)}$, being faster in native and DE(L213) RCs and slower in DN(L213) RCs. The amplitude of this uptake is greater in the DN(L213) RCs compared to native RCs, probably because the change in the protonation state of Glu-L212 upon Q_B reduction is greater in the DN(L213) RCs at the measured pH 7.5. This is an expected consequence of a reduced pK_a for Glu-L212 in the DN(L213) RCs (pK_a ≲ 8)

[3] The pH profile for the DN(L213) RCs is similar to that reported by Takahashi and Wraight (1992) except the rates reported here are slower for pH > 6.5. This difference is due to the type of exogenous donors used in the two experiments; they used ferrocene and we used cyt *c*. The rates we measured by monitoring semiquinone decay using ferrocene were anomalously fast at higher pH, presumably because of electron leakage from $DQ_A^-Q_B^-$ to solution (Takahashi & Wraight, 1992) and not due to the forward electron transfer $k_{AB}^{(2)}$.

[4] The dependence of the observed rate on pH reported here at high pH differ from those reported by Kleinfeld *et al.* (1984). We believe this to be a consequence of the experimental conditions. In this work, we use excess UQ_{10} in our samples, which drives the second electron transfer to completion. Hence the observed rate is the forward electron transfer rate. Kleinfeld *et al.* used a sample that contained no excess quinone; thus the observed rate in that work is the sum of the forward and back rate constants. Our results agree well with the forward rate $k_{AB}^{(2)}$ reported in Figure 6 of Kleinfeld *et al.* (1984).

[5] The rate measured in DE(L213) RCs without excess quinone was found to be the same with similar amplitudes, suggesting that the slow observed rate is due to slow forward electron transfer and not quinone/quinol exchange (see footnote 4).

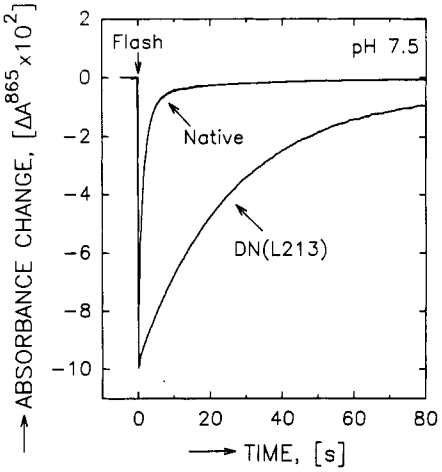

FIGURE 6: Charge recombination kinetics, k_{BD}, monitored *via* the absorbance of the donor at 865 nm as a function of time at pH 7.5. The slower rate of charge recombination in the DN(L213) RCs compared to the rate in native RCs suggests a more stable $D^+Q_AQ_B^-$ state in the mutant RCs. The charge recombination kinetics are similarly slowed in the DE(L213), DL(L213), DS(L213), and DT(L213) RCs (see text, Table 1). The slower rate of recovery is attributed to the removal of a predominant negatively charged Asp in the mutant RCs. (Conditions: ~1 μM RC in HMK buffer, 1 μM ferricyanide, 23 °C.)

compared to the native RCs ($pK_a \sim 9$) and the strong interaction between Q_B^- and Glu-L212 (see later discussion).

The observed proton uptake by native RCs (Figure 5a) after the second flash due to the reaction $DQ_A^-Q_B^- \rightarrow DQ_AQ_BH_2$ was rapid and not resolved in the figure ($k = 1200$ s^{-1}). The total proton uptake after both flashes had a value of 2.0 H^+/Q_B^{2-} after correction of the observed value for the proton release from the oxidized cyt *c* (~ 0.1 H^+/RC) for the small fraction of RCs that lacked a bound Q_B (~0.1 H^+/RC) and for the equilibrium fraction (~10%) of RCs in the $DQ_A^-Q_B$ state after the first flash (McPherson *et al.*, 1993a).

In the DN(L213) RCs the proton uptake rate after the second laser flash was biphasic (Figure 5b). The slow phase had a rate of 0.23 s^{-1} and corresponded to the uptake of ~1 H^+/Q_B^{2-} after corrections. The rate of the slow proton uptake was, within experimental error, equal to the observed rate of the electron/proton transfer reaction $Q_A^-Q_B^- + H^+ \rightarrow Q_AQ_B^{2-}H^+$ in the DN(L213) RCs and was also equal to half the cytochrome turnover rate, as expected if all three measurements were limited by the same process. The fast phase is attributed to the partial proton uptake that results from pK_a shifts of nearby amino acid residues due to the reduction of the quinone molecules (Maróti & Wraight, 1988; McPherson *et al.*, 1988).

The rate observed in the DE(L213) RCs (not shown) was slower than observed in native RCs but faster than observed in the DN(L213) RCs and was consistent with the rate of the electron/proton transfer reaction $Q_A^-Q_B^- + H^+ \rightarrow Q_AQ_B^{2-}H^+$ ($k \sim 16$ s^{-1}).

Charge Recombination Rates. The charge recombination rates contain important information about the electrostatic environment around the reduced quinone molecules. The charge recombination rates $D^+Q_A^- \rightarrow DQ_A$ (k_{AD}) and $D^+Q_AQ_B^- \rightarrow DQ_AQ_B$ (k_{BD}) were measured by monitoring the change in absorption of the primary electron donor at 865 nm (Table 1).

(*A*) k_{AD}:$D^+Q_A^- \rightarrow DQ_A$. The recombination rate k_{AD}, measured in RCs containing only one quinone (Q_A), was found to be essentially the same in the native and in the DN(L213), DL(L213), DS(L213), DT(L213), and DE(L213) mutant RCs ($k_{AD} \sim 10$ s^{-1}).

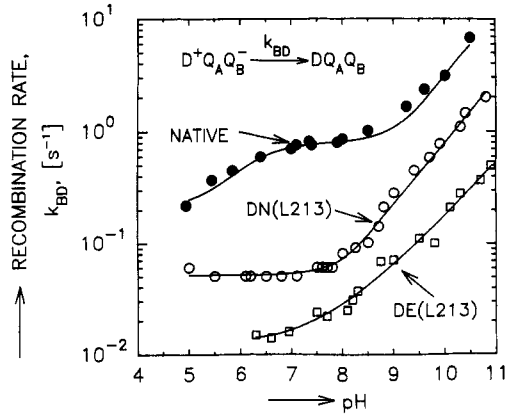

FIGURE 7: pH dependence of the charge recombination rate, k_{BD}, determined as described in Figure 6 for native, DN(L213), and DE(L213) RCs. The smaller values of k_{BD} measured in the DN(L213) and DE(L213) RCs near pH 7 suggests that Asp-L213 is negatively charged in native RCs and is replaced with neutral residues (*e.g.*, Asn or Glu) in the mutant RCs. The increase at high pH ≥ 8 was shown to be related to the titration of Glu-L212 in native RCs (Paddock *et al.* 1989). Note that the pH at which k_{BD} starts to increase is shifted in the mutant RCs. This is consistent with the replacement of a negatively charged Asp-L213 with neutral Asn or Glu, shifting the apparent pK_a of Glu-L212 by 1–2 units. In the DE(L213) RCs, Glu-L213 could also contribute to the pH dependence at pH > 7. Thus, the pK_a of Glu-L213 appears to be ≥7. (Conditions: ~2 μM RCs; 2 mM each Hepes, Caps, Ches, Mes, Pipes, and Tris; 0.04% dodecyl β-D-maltoside; 50 mM KCl; 23 °C, 1 μM ferricyanide.) The pH was adjusted by adding HCl or NaOH.

(*B*) k_{BD}:$D^+Q_AQ_B^- \rightarrow DQ_AQ_B$. The recombination rate k_{BD} was measured in the presence of excess UQ_{10} (~5–10 UQ_{10}/RC). It was determined from the kinetics of the slow phase of D^+ recovery at 865 nm (Figure 6). The k_{BD} values of all the mutant RCs[6] (Table 1) were significantly smaller ($k_{BD} \leq 0.04$ s^{-1}) than those of the native ($k_{BD} = 0.7$ s^{-1}). A minor fraction (~20%) of the DE(L213) RCs had a larger k_{BD} (~0.25 s^{-1}) than the major phase.

The smaller values of k_{BD} in the mutant RCs indicate that Q_B^- is stabilized in the mutant RCs. Analysis of the data leads to an estimated stabilization of Q_B^- by ≥60 meV [see, *e.g.*, Kleinfeld *et al.* (1984)]; thus the equilibrium fraction of $Q_A^-Q_B$ is decreased. This results in k_{BD} proceeding by direct charge recombination below pH 8 (Labahn *et al.*, 1994).

The pK_a values of Asp-L213 and Glu-L213 were estimated [see, *e.g.*, Kleinfeld *et al.* (1984)] from the pH dependence of k_{BD} (Figure 7), which is sensitive to the charges near Q_B, *i.e.*, the ionization states of all charged species near Q_B including L213. Native RCs show two pH-dependent regions: one at pH > 9 and the other at pH < 7. In the DN(L213), DL(L213), DS(L213), DT(L213), and DE(L213) RCs, the onset of the high-pH dependence was shifted from pH ~ 9 to pH ~ 8. Below pH 8, k_{BD} in all mutant RCs was found to be essentially independent of pH, showing that Asp-L213 is important for the low-pH region titration. The pK_a of Asp-L213 is estimated to be below 4 on the basis of analysis of similar data (Takahashi & Wraight, 1990; Paddock *et al.* 1991a; Okamura & Feher, 1992). The DE(L213) RCs were unstable below pH ~ 6; consequently k_{BD} could not be measured in this mutant below pH 6.

[6] The rates reported here are approximately 1.5–2-fold slower than those reported by Takahashi and Wraight (1990, 1991, 1992). This may be a result of different experimental conditions, *e.g.*, detergent, light intensity of the monitoring beam. Because of the great stability of the charge-separated state, we had to greatly reduce the light intensity of the monitoring beam ≥5-fold for the mutant RCs compared to that used for native RCs to obtain a charge recombination rate that was independent of light intensity.

In the DE(L213) RCs, near neutral pH, Glu-L213 is presumably protonated (neutral) as deduced from the small observed k_{BD} values, with an apparent pK_a near 7. Thus the pK_a difference between Asp-L213 and Glu-L213 is ≥3 pK_a units, much larger than the 0.4 pK_a unit difference observed in solution (Edsall & Wyman, 1958).

(C) Effect of Azide on k_{BD}. Binding of charged groups in the vicinity of Q_B^- is expected to affect the recombination kinetics (k_{BD}). Consequently, we used the measurement of k_{BD} as an assay for azide binding. The value of k_{BD} in DN(L213) RCs increased with increasing azide concentration, with a maximum 2.2-fold increase at 1 M azide (pH 7.5) (data not shown). The increase of the rate (as a percentage of the maximum increase) at any azide concentration was essentially the same for either k_{BD} or $k_{AB}^{(2)}$. The data are consistent with a weak binding of N_3^- to the RC. Essentially no enhancement in the rates was observed upon addition of NaCl up to a concentration of 1 M. Similarly, essentially no effect (<20% decrease) was observed in the native and DE(L213) RCs upon addition of azide or NaCl up to 1 M concentration.

DISCUSSION

Importance of Asp-L213 in Proton Transfer Reactions: (A) Proton Transfer Associated with the First Electron Transfer $k_{AB}^{(1)}$. The kinetics of the first electron transfer $k_{AB}^{(1)}$ ($D^+Q_A^-Q_B \rightarrow D^+Q_AQ_B^-$) when Asp-L213 was replaced with Asn, Leu, Ser, or Thr was slowed ~10-fold at pH 7.5 [see DN(L213) in Table 1], despite the fact that this reaction in the mutant RCs is thermodynamically more favorable due to the lowering of the energy of the $Q_AQ_B^-$ state (see results of k_{BD} measurements). The reduction of $k_{AB}^{(1)}$ in the DN(L213) mutant RCs has been attributed to a slow rate-limiting protonation step (McPherson *et al.*, 1991; Takahashi & Wraight, 1992, 1993; Shinkarev *et al.*, 1992), presumably of Glu-L212 (McPherson *et al.*, 1991). The reduction in $k_{AB}^{(1)}$ following the replacement of Asp-L213 with Asn suggests that proton transfer to Glu-L212 proceeds through a pathway influenced by Asp-L213, either as a proton transfer component or affecting the energetics of other proton transfer components. The faster $k_{AB}^{(1)}$ observed in the DE(L213) RCs (Table 1) is consistent with the observed faster proton uptake in this mutant and adds support to the proposal that Asp-L213 is involved in proton transfer to Glu-L212.

(B) Proton Transfer Associated with the Second Electron Transfer $k_{AB}^{(2)}$. The proton-coupled electron transfer $k_{AB}^{(2)}$ ($DQ_A^-Q_B^- + H^+ \rightarrow DQ_AQ_BH^-$) was reduced ~6000-fold when Asp-L213 was replaced with Asn, Leu, Ser, or Thr compared to native RCs and ~70-fold when Asp-L213 was replaced with Glu. These kinetic results show a correlation between the presence of a carboxylic acid at the L213 site and an effective proton-coupled electron transfer $k_{AB}^{(2)}$. The faster rates observed in RCs with either Asp-L213 or Glu-L213 suggest that each of these residues constitutes a component of a proton transfer chain. Additional evidence for this comes from the crystal structure, which suggests that Asp-L213 is part of a proton transfer chain leading from solution to Ser-L223 and Q_B in native RCs (Allen *et al.*, 1988; Beroza *et al.*, 1992). However, the possible importance of the electrostatics associated with the L213 site on proton transfer reactions should also be considered, especially in light of the recent observation that proton transfer to reduced Q_B was increased by reduction of Q_A by up to 8-fold (pH 6) in RCs where Glu-L212 was replaced with Gln (McPherson *et al.*, 1993b).

To investigate the electrostatic environment around Q_B^-, the charge recombination kinetics k_{BD} ($D^+Q_AQ_B^- \rightarrow DQ_AQ_B$) provides a convenient and useful assay [see, *e.g.*, Kleinfeld *et al.* (1984)]. As a negative charge is removed (or a positive charge is introduced), k_{BD} decreases, indicating a stabilization of Q_B^-. Likewise, as a negative charge is introduced, k_{BD} increases. Thus the smaller values of k_{BD} in the mutant RCs (Table 1) imply that a negative charge has been removed in the vicinity of Q_B^- when Asp-L213 was replaced with Asn, Leu, Ser, Thr, or Glu. This alteration in the electrostatic environment can affect proton transfer reactions.

Several arguments suggest the importance of the electrostatic influence of Asp-L213 on internal proton transfers. First, there is a general correlation in the mutant RCs between a small value of k_{BD} and a small value of $k_{AB}^{(2)}$ (see Table 1). This suggests that an environment that stabilizes Q_B^- inhibits proton transfer to reduced Q_B. This seems reasonable since a charge change that stabilizes a negatively charged species like Q_B^- will destabilize a positively charged species like H^+ and *vice versa*. Second, a double mutant containing Asp-L213 → Asn/Arg-M233 → Cys displays larger values of k_{BD} and $k_{AB}^{(2)}$ compared to RCs with the single Asp-L213 → Asn replacement (Rongey *et al.* unpublished results). The larger $k_{AB}^{(2)}$ is not likely due to the introduction of a new proton transfer pathway since Arg-M233 is quite distant (≥17 Å) from Asp-L213. It is more likely that the altered electrostatic environment, as evidenced by the larger k_{BD} value, favors internal proton transfer reactions and hence increases $k_{AB}^{(2)}$. Third, the addition of azide (N_3^-) to RCs with Asn, Leu, Ser, or Thr simultaneously increases k_{BD} and $k_{AB}^{(2)}$ in a similar concentration-dependent manner.

Although the results clearly show that Asp-L213 is crucial for the proton-coupled electron transfer $k_{AB}^{(2)}$, the relative importance of its dual roles—as a proton transfer agent and in establishing a favorable electrostatic environment—is at present not clear. Several studies are in progress to elucidate this point. Reaction centers are being constructed in which Asp-L213 is replaced with other proton donor groups, *e.g.*, His, Lys, and Cys. In addition, combining the changes discussed above with a compensating change that retains a similar electrostatic environment around Q_B^- may lead to more definitive conclusions about the relative importance of the dual roles of Asp-L213. Finally, employing the techniques of Fourier transform infrared difference spectroscopy (Breton *et al.*, 1991a,b) and kinetic infrared spectroscopy (Hienerwadel *et al.*, 1992) on native and mutant RCs could determine if Asp-L213 changes protonation state during electron transfer processes [see, *e.g.*, Hienerwadel *et al.* (1993)].

Mode of Action of Azide in Bacterial RCs. Azide increases the proton transfer rate in halorhodopsin (Hegemann *et al.*, 1985; Lanyi, 1986) and mutants of bacteriorhodopsin (Tittor *et al.*, 1989). The addition of azide to RCs in which Asp-L213 was replaced with Asn, Leu, Ser, or Thr increased $k_{AB}^{(2)}$ by up to ~40-fold at 1 M (pH 7.5), but this is still 100-fold slower than native rates. Takahashi and Wraight (1991) also found that azide and other weak acids increased the observed $k_{AB}^{(2)}$ in DN(L213) RCs from *Rb. sphaeroides* and interpreted their results in terms of the known protonophore activity of azide.

We favor an interpretation in which the effect of azide is attributed to an electrostatic interaction. Evidence for this is provided by the effect of azide on the charge recombination kinetics (see results). Although the effect on k_{BD} is significantly smaller than that on $k_{AB}^{(2)}$, the functional dependence of k_{BD} on azide concentration (*i.e.*, the percent of the maximum effect as a function of azide concentration) is nearly identical to that observed for $k_{AB}^{(2)}$. The fact that essentially no effect was observed upon addition of NaCl suggests that the effect

is not due solely to dielectric screening. The simplest interpretation of these results is that N_3^- binds weakly to the RC, whereas Cl^- essentially does not bind. The binding of N_3^- can increase the observed $k_{AB}^{(2)}$ through the introduction of a negative charge near Q_B, thus favoring proton transfer. Therefore, azide may function by restoring a negative charge near L213 in these mutant RCs rather than as a protonophore.

Other Proton Transfer Pathway(s) Not Involving Asp-L213. In RCs where Asp was replaced with Asn, Leu, Ser, or Thr, proton transfer to reduced Q_B proceeds, albeit at a slow rate. Asn, Leu, Ser, and Thr are not able to substitute for Asp in proton transfer reactions so presumably a slower, alternate, pathway takes over. It is, however, possible to provide in the Asp-L213 mutant RCs an alternate, efficient, proton transfer path(s) by making compensating mutations. One example is the replacement of Asn-M44 with Asp. A functionally active double mutant was constructed in *Rb. sphaeroides* (Asp-L213 → Asn/Asn-M44 → Asp) where the position of Asp was moved from L213 to M44 (Rongey *et al.*, 1993). These RCs displayed near native rates for $k_{AB}^{(2)}$ and k_{BD}. Similarly, a compensating suppressor mutation of *Rhodobacter capsulatus* (Asp-L213 → Ala/Glu-L212 → Ala/Asn-M43 → Asp) (Hansen *et al.*, 1992a) displayed some restoration of the rates (although not quantified).

A second example is a compensating change at Arg-M233 in *Rb. sphaeroides* (Asp-L213 → Asn/Arg-M233 → Cys) (Feher *et al.*, 1992; Okamura *et al.*, 1992[7]) or *Rb. capsulatus* (Asp-L213 → Ala/Glu-L212 → Ala/Arg-M231 → Leu) (Hansen *et al.*, 1992b). The site of compensation is located ≥17 Å from the L213 site. In *Rb. sphaeroides* the mutant RCs display reduced (~30-fold at pH 7.5) values for $k_{AB}^{(2)}$ compared to native RCs and slightly faster (2-fold at pH 7.5) charge recombination kinetics k_{BD}. The partial restoration of $k_{AB}^{(2)}$ over that seen in the parent strain (Asp-L213 → Asn) can be explained by a change in the electrostatic environment near Q_B^- that enhances the proton transfer rate of an existing pathway, whereas in the previous examples an alternate proton transfer pathway may have been created.

Why Are the Observed pK_a Values of Asp-L213 and Glu-L213 So Different? The difference in the pK_a values between Asp-L213 in native RCs and Glu-L213 in DE(L213) mutant RCs is ≥3 pK_a units (see results), whereas the difference in their pK_a values in aqueous solution is only 0.4 pK_a unit (Edsall & Wyman, 1958). We believe that the major contribution to this large difference arises from the electrostatic interaction of Asp and Glu with nearby residues. We show in the Appendix that if two residues interact electrostatically, then the observed pK_a[8] difference, ΔpK^{obs}, will be increased by the interaction term ΔpK_a^{inter}:

$$\Delta pK_a^{obs} = \Delta pK_a^{sol} + \Delta pK_a^{inter} \quad (1)$$

where ΔpK_a^{sol} is the expected difference with no interactions (*i.e.*, in solution).

We next discuss with the aid of a model how an interaction with a nearby residue can affect the titration of Asp-L213 and Glu-L213 so differently. Although there are at least three residues (Glu-L212, Asp-L213, and Asp-L210) that interact strongly [reviewed in Okamura and Feher (1992)], we shall simplify the situation by considering only the strongly coupled Asp-L213 and Asp-L210 residues (located ~3 Å apart in the RC; Allen *et al.*, 1988). If

$$pK_a(\text{Asp-L213}) = 3.0, \quad pK_a(\text{Asp-L210}) = 3.3, \quad \text{and} \quad \Delta pK_a^{inter} = 3.0 \quad (2)$$

then the observed pK_a values will be (eq 1)

$$pK_a^{obs}(\text{Asp-L213}) = 3.0 \quad \text{and} \quad pK_a^{obs}(\text{Asp-L210}) = 6.3 \quad (3)$$

If the pK_a of Glu-L213 is only 0.5 pK_a unit higher than that of Asp-L213 (a difference near that found in solution), the order of ionization of the L213 and L210 pair will be reversed, *i.e.*, for

$$pK_a(\text{Glu-L213}) = 3.5, \quad pK_a(\text{Asp-L210}) = 3.3, \quad \text{and} \quad \Delta pK^{inter} = 3.0 \quad (4)$$

the observed pK_a values will be

$$pK_a^{obs}(\text{Glu-L213}) = 6.5 \quad \text{and} \quad pK_a^{obs}(\text{Asp-L210}) = 3.3 \quad (5)$$

This illustrative example predicts a difference in the observed pK_a between Asp-L213 and Glu-L213 of 3.5 pK_a units, similar to that observed.

It is interesting to note that the large difference in the pK_a values between Glu and Asp at the same position has been observed at other positions in the RC and in other membrane-bound proteins, *e.g.*, at the L212 site in *Rb. sphaeroides* ($\Delta pK_a^{obs} \geq 4$ units) (Paddock *et al.*, 1990b) and at the 85 site in bacteriorhodopsin ($\Delta pK_a^{obs} \geq 4$ units) (Subramaniam *et al.*, 1990). Perhaps the large ΔpK_a^{obs} is a general feature of acid residues in membrane proteins. It should be noted that, in addition to the effect discussed above, other factors could contribute to the difference in the observed pK_a values between Asp and Glu, *e.g.*, (i) a decreased electrostatic interaction between Glu-L213 and nearby fixed charges like Arg-L217 or fixed dipoles such as those associated with the protein helices or (ii) steric restrictions due to the greater length of Glu over Asp that could change the solvation.

Models of the Proton-Coupled Electron Transfer $k_{AB}^{(2)}$. The transfer of the *second* electron to Q_B is coupled with the binding of the *first* proton as illustrated by the $k_{AB}^{(2)}$ reaction in eq 6 [see also Maróti and Wraight (1990) and Okamura and Feher (1992)]. The second proton transfer $H^+(2)$ is taken up after electron transfer as indicated by the characteristics of RCs with Glu-L212 replaced by Gln (Paddock *et al.*, 1989; Takahashi & Wraight, 1992) or Asp (Paddock *et al.*, 1989).

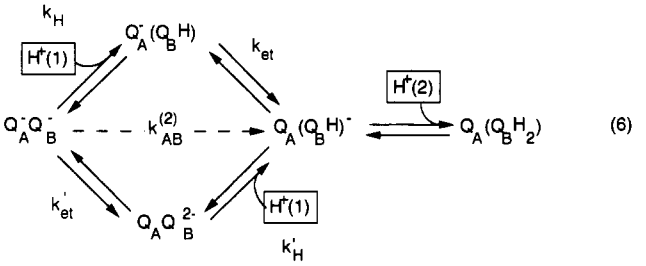

(6)

The $k_{AB}^{(2)}$ reaction can proceed *via* either of the two reaction paths shown in eq 6. In the upper reaction, proton transfer precedes electron transfer with the formation of the transient protonated semiquinone state Q_BH. In the lower reaction, electron transfer precedes proton transfer with the formation of the transient dianionic state Q_B^{2-}. In either reaction path the rate-limiting step may be either the proton transfer k_H (or k_H') or the electron transfer k_{et} (or k_{et}'). Since the microscopic rates for the individual steps have not been established, we have, in principle, four different possible cases. We shall discuss them in turn below.

[7] There is an error in the title of the article. It should read "Proton Transfer in Bacterial Reaction Centers: Second Site Mutations Asn-M44 → Asp or Arg-M233 → Cys Restore Photosynthetic Competence to Asp-L213 → Asn Mutation in RCs from *Rb. sphaeroides*."

[8] With interacting residues the classic definition of pK_a^{obs} no longer applies. Here our functional definition of pK_a^{obs} is the pH at which the slope of the fraction of protonated acid versus pH reaches its maximum.

Case 1: Upper Path in Equation 6 with $k_H \ll k_{et}$. In this model, the rate-limiting step is the internal proton transfer that precedes electron transfer. The observed rate will depend on this internal proton transfer between components of the proton transfer chain (*e.g.*, between Asp-L213 and Ser-L223). We shall try to estimate the proton transfer from Asp-L213 (or Glu-L213) to Ser-L223 to see if it corresponds to the observed value.

Proton transfer in proteins is generally believed to involve a chain of proton donor/acceptor groups, *e.g.*, amino acid residues or water molecules (Nagle & Tristram-Nagle, 1983; Schulten & Schulten, 1986; Warshel, 1986). The ability of a residue, *e.g.*, Asp-L213, to function as part of a proton transfer chain is related to its pK_a. The rate for activated (energetically unfavorable) proton transfer from a proton donor group (D) to an acceptor group (A) within hydrogen-bonding distance can be estimated from the relation

$$k_H = k_0 10^{-[pK_a(D) - pK_a(A)]} \quad (7)$$

where pK_a(D) is the pK_a of the donor group, pK_a(A) is the pK_a of the acceptor, and k_0 is 10^{12}–10^{13} s^{-1} (Warshel, 1986; Gutman & Nachliel, 1990). The pK_a values are assumed to be constant during the proton transfer, although in practice they may vary due to an altered electrostatic environment upon proton transfer. Since k_0 is large, even energetically unfavorable proton transfer can be fast enough to account for the observed proton-coupled electron transfer rate in RCs (*e.g.*, $k_{AB}^{(2)} = 10^3$ s^{-1} at pH 7.5). For example, the transfer of a proton from Asp-L213, with an estimated p$K_a \sim 6$, to Ser-L223, with a pK_a of –2 in solution, could occur at a rate of 10^4–10^5 s^{-1}.

The proton transfer from Asp-L213 (or Glu-L213) to Ser-L223 is given by the proton transfer rate k_H (eq 7) times the fraction of protonated Asp-L213 (or Glu-L213), f_H(L213):

$$k_{AB}^{(2)} = k_H f_H(\text{L213}) = k_0 10^{-[pK_a(D) - pK_a(A)]} f_H(\text{L213}) \quad (8)$$

where

$$f_H(\text{L213}) = \frac{1}{1 + 10^{pH - pK_a(\text{L213})}} \quad (9)$$

We shall compare now the experimentally observed values of $k_{AB}^{(2)}$ for both the native and DE(L213) RCs and their respective pH dependences with the theoretical predicted values given by eq 8.

The ratio of $k_{AB}^{(2)}$ [DE(L213)]/$k_{AB}^{(2)}$ [native] when both Asp-L213 and Glu-L213 are fully protonated, *i.e.*, f_H(L213) = 1, should equal $10^{-\Delta pK_a^{obs}}$, where ΔpK_a^{obs} is the difference in pK_a between Glu-L213 and Asp-L213, estimated to be ≥3 units (see previous section on k_{BD}). Thus, at low pH we expect $k_{AB}^{(2)}$ to be at least 3 orders of magnitude larger in native RCs than in the DE(L213) RCs. Inspection of Figure 4 shows that, at pH 4, $k_{AB}^{(2)}$ of the native RCs is approximately 3 orders of magnitude larger than in the DE(L213) RCs, in good agreement with the prediction.

We next turn to the pH dependence of $k_{AB}^{(2)}$. It arises from the titration of L213, *i.e.*, f_H(L213) in eq 8. The data of the DE(L213) are fitted with a pK_a^{obs}(Glu-L213) = 9, the pH at which $k_{AB}^{(2)}$ reaches half its asymptotic value. The pH dependence of the native RCs is not as straightforward, presumably because of interactions with other titrating residues. However, it does not seem unreasonable to assign to it a pK_a^{obs}(Asp-L213) = 6, giving the same ΔpK_a used in the previous section. It should be noted that the pK_as determined here are for the ionized quinone state $Q_A^- Q_B^-$, whereas the pK_as discussed in the previous section were for the neutral quinone state $Q_A Q_B$. That the ΔpK_as are the same (~3 pK_a units) for the two cases indicates that the electrostatic interactions of Q_B^- with ionized Asp-L213 and ionized Glu-L213 are the same.

To calculate the absolute value of $k_{AB}^{(2)}$, we fit eq 8 to the observed value for $k_{AB}^{(2)}$ using pK_a(A) as an adjustable parameter. For the DE(L213) RCs, $k_{AB}^{(2)} \sim 10$ s^{-1} (see Figure 4), $k_0 = 10^{12}$–10^{13} s^{-1}, and pK_a^{obs}(Glu-L213) = 9. Substituting these values into eq 8 yields

$$pK_a(\text{A}) = -2 \text{ to } -3 \quad (10)$$

This is close to the solution p$K_a \sim -2$ of the ROH_2^+ state of Ser (Stewart, 1985) and is consistent with the suggestion that the observed $k_{AB}^{(2)}$ could be limited by an internal proton transfer step with Ser-L223 as the proton acceptor. This is consistent with previous results on site-directed mutations (Paddock *et al.*, 1990) and herbicide resistant mutations (Leibl *et al.*, 1993) that suggested the importance of Ser-L223 for proton transfer to reduced Q_B.

Case 2: Upper Path in Equation 6 with $k_{et} \ll k_H$. In this case the rate-limiting step is electron transfer, which follows proton transfer. The faster proton transfer establishes an equilibrium between Q_B^- and Q_BH. The rate $k_{AB}^{(2)}$ will be proportional to the fraction of protonated semiquinone, $f_H(Q_B)$, and the electron transfer rate k_{et}:

$$k_{AB}^{(2)} = k_{et} f_H(Q_B) \quad (11)$$

We assume no pH dependence of k_{et}. Thus the pH dependence of $k_{AB}^{(2)}$ arises from the fraction of protonated semiquinone, $f_H(Q_B)$, which will be affected by electrostatic interactions with nearby residues. We shall simplify the problem by using two titrating interacting residues Q_BH and Asp-L213 (or Glu-L213) (see Appendix).

For native RCs the observed pH dependence of $k_{AB}^{(2)}$ (Figure 4) is consistent with the following parameters:

$$\Delta pK_a^{inter} = 3.5, \quad pK_a(Q_BH) = 3, \quad pK_a(\text{Asp-L213}) = 3,$$

$$\text{and} \quad k_{et} = 10^4 \text{ s}^{-1} \quad (12)$$

where k_{et} was obtained from the asymptotic (low-pH) value of $k_{AB}^{(2)}$.

For the DE(L213) RCs, the data are consistent with the same set of parameters replacing pK_a(Asp-L213) with pK_a(Glu-L213) = 6, *i.e.*, 3 pK_a units higher than pK_a(Asp-L213) as discussed above. The observed pK_a of Glu-L213 would be 3.5 pK_a units larger, pK_a^{obs}(Glu-L213) ~ 9.5, due to the interaction between Glu-L213 and Q_B^- (see Appendix). This is in agreement with the observed decrease in $k_{AB}^{(2)}$ for pH ≥ 9.5, when the concentration of Q_BH depends strongly on pH [see Appendix, Figure 9a, $pK_a(2) = 6$]. The observed rate is expected to be pH-independent in the region between pK_a(Glu-L213) and pK_a(Glu-L213) + ΔpK_a^{inter}, *i.e.*, 6 ≤ pH ≤ 9.5, as is observed (see also Appendix, eq A1). In this pH range, approximately one proton is shared between the two titrating sites with the relative protonation of Q_BH to L213 given by $10^{pK_a(QH) - pK_a(L213)}$. The reduced value of $k_{AB}^{(2)}$ observed in the DE(L213) RCs compared to native RCs is due to a smaller fraction of Q_BH, reduced by ~10^3, caused by the higher pK_a(Glu-L213) compared to pK_a(Asp-L213) (by 3 pK_a units). Thus the relative difference between native and DE(L213) $k_{AB}^{(2)}$ values, pH dependences, and absolute values can be explained for this case as well.

Case 3: Lower Path in Equation 6 with $k_H' \ll k_{et}'$. This is similar to case 1 discussed above except that the rate-limiting proton transfer step follows electron transfer (lower path of eq 6). $k_{AB}^{(2)}$ will be proportional to the fraction of doubly

reduced quinone $f(Q_B^{2-})$:

$$k_{AB}^{(2)} = f(Q_B^{2-})k_H f_H(L213) \quad (13)$$

where k_H is given by eq 7 and $f_H(L213)$ is given by eq 9. The value of $f(Q_B^{2-})$ was assumed to be independent of pH. Thus the predicted pH dependence is due to the titration of Asp-L213 (or Glu-L213), the same as that predicted by case 1 discussed above. The ratio $k_{AB}^{(2)}[DE(L213)]/k_{AB}^{(2)}[native]$ should equal $10^{-\Delta pK_a^{obs}}$ times the ratio $f(Q_B^{2-})[DE(L213)]/f(Q_B^{2-})[native]$. It is likely that $f(Q_B^{2-})$ is increased in the DE(L213) RCs by at least 1 order of magnitude, since the altered electrostatic environment in the DE(L213) RCs favors reduction of Q_B as illustrated by the small values for k_{BD} (Figure 7, see discussion above). Using $\Delta pK_a^{obs} = 3$ (as discussed for case 1), one estimates in the low-pH limit where $f_H(L213) \sim 1$ a ratio of $\geq 10^{-2}$, which is larger than the observed ratio of 10^{-3}. However, the results can still be considered in fair agreement with observation given the simplified assumptions used in this analysis.

To calculate the absolute value of $k_{AB}^{(2)}$, we fit eq 13 to the observed value for $k_{AB}^{(2)}$ using $pK_a(A)$ as an adjustable parameter and assuming values for $f(Q_B^{2-})$. A reasonable maximum limit for $f(Q_B^{2-})$ can be obtained from the cytochrome photooxidation data. The rate of formation of the $Q_A^-Q_B^{2-}$ state can be driven by continuous illumination since those RCs in the $DQ_AQ_B^{2-}$ state given by $f(Q_B^{2-})$ can undergo additional photochemistry. This will give rise to a difference between the photocycle rate (measured in the presence of continuous illumination) and $k_{AB}^{(2)}$ (measured with short laser pulses). This difference is proportional to $f(Q_B^{2-})$ and the excitation rate of the RCs:

$$k_{cycle} - k_{AB}^{(2)} = f(Q_B^{2-})k_I \quad (14)$$

where k_{cycle} is the photocycle rate and k_I is the number of photons per second absorbed by the RCs $\simeq 10^3$ s^{-1}, the excitation rate of native RCs measured under identical conditions. Using the values of the photocycle rate and $k_{AB}^{(2)}$ found in Table 1, one estimates a value of $f(Q_B^{2-}) \sim 2 \times 10^{-3}$.[9] Given the error in the measured values, $f(Q_B^{2-})$ could be zero, so this value should be viewed as an upper estimate for $f(Q_B^{2-})$. Nevertheless, for $f(Q_B^{2-}) = 2 \times 10^{-3}$, $k_{AB}^{(2)}$ can be fitted with eq 13 using $pK_a(A) = 0$–1, which is close to the pK_a value for the ROH_2^+ state of Ser in solution (Stewart, 1985). This pK_a value could be altered in the RC due to interactions with nearby charges [see, *e.g.*, Okamura and Feher (1992)].

Case 4: Lower Path in Equation 6 with $k_{et}' \ll k_H'$. This case can be excluded by comparing the values of $k_{AB}^{(2)}$ and k_{BD} of the native (Asp-L213) and the DE(L213) RCs. The value of k_{BD} in the DE(L213) mutant RCs is ~15-fold smaller than in native RCs (see Figure 7), showing that the state $Q_AQ_B^-$ is energetically lower in the mutant RCs. This increases the driving force for electron transfer from the Q_A^- state. On the basis of previous observations of $k_{AB}^{(1)}$ in herbicide-resistant mutants (Paddock *et al.*, 1991b), this should result in an increase in k_{et}' and thus $k_{AB}^{(2)}$, contrary to what is observed (see Figure 4).

The first three cases discussed above predict semiquantitatively the observed values and pH dependence of $k_{AB}^{(2)}$ for native and DE(L213) RCs. To distinguish between them, additional experiments and analyses need to be performed. For example, observation of either Q_BH or Q_B^{2-} as an intermediate (eq 6) can eliminate at least one of the models discussed above.

[9] This maximum value for $f(Q_B^{2-})$ of 2×10^{-2} can be used to estimate a minimum value of ΔG^0[DE(L213)] between the $Q_AQ_B^{2-}$ and $Q_A^-Q_B^-$ states of +160 meV using $\Delta G^0 = -2.3kT \log\{f(Q_B^{2-})/[1 - f(Q_B^{2-})]\}$ [see, *e.g.*, Kleinfeld *et al.* (1985)]. This value would be greater in native RCs, increased by the interaction energy between a charge at L213 and Q_B^- of $\geq$ 60 meV to give ΔG^0(native) $\gtrsim$ +220 meV.

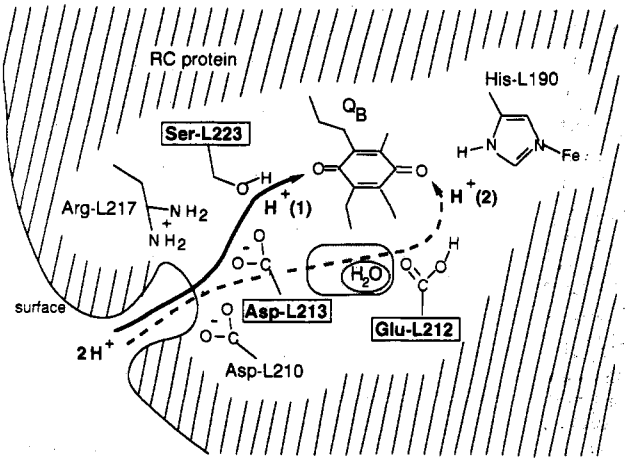

FIGURE 8: Molecular model of proton transfer in the bacterial RC from *Rb. sphaeroides* based on the results discussed above and the crystal structure by Allen *et al.* (1988). The relative positions of several amino acid residues are shown. The interior of the protein is indicated (hatched). The results from these experiments have been used to extend a previously proposed molecular model for the proton transfer events (Paddock *et al.*, 1990). The first proton [H^+(1)] that is important for the transfer of the second electron reduction of Q_B (eq 2a) is transferred from an aqueous donor to Asp-L213 and then to Ser-L223 and reduced Q_B. This transfer might be catalyzed by Asp-L210 and Arg-L217, although there is no firm evidence to support this possibility. The second proton [H^+(2)] is proposed to be transfered from the surface to Glu-L212 and onto reduced Q_B. The replacement of Asp-L213 with Asn reduces the rate of protonation of Glu-L212 in the DN(L213) RCs; thus Asp-L213 is believed to play a role in this proton transfer event. Bound water may mediate protonation of Glu-L212 since it is quite distant from other protonatable residues (*e.g.*, 7 Å from Asp-L213). Modified from Feher *et al.* (1992) and Okamura and Feher (1992).

Proton Transfer Pathways in Bacterial RCs. Our current model for proton transfer to reduced Q_B (Figure 8) in native RCs from *Rb. sphaeroides* is based on the results discussed in this work as well as previous results from site-directed mutagenesis experiments and inspection of the three-dimensional crystal structure. It has been discussed in detail elsewhere (Feher *et al.*, 1992; Okamura & Feher, 1992) and will be updated and reviewed briefly below.

Reduction of Q_B to Q_BH_2 involves the sequential transfer of two electrons and two protons (Figure 1 and eq 6). The first proton transfer to reduced Q_B [H^+(1) in eq 6 and Figure 8] involves Ser-L223 (Paddock *et al.*, 1990a) and probably Asp-L213.

Evidence for the involvement of Asp-L213 in proton transfer was discussed in this work. Protons, possibly carried by water molecules, may permeate the protein to a region near Asp-L213 (Beroza *et al.*, 1992). The crystal structure (Allen *et al.*, 1988) suggests that proton transfer may occur from Asp-L213 to Ser-L223 (~3 Å apart) and then through the hydrogen bond from Ser-L223 to reduced Q_B (~3 Å apart). In some bacteria, the native Asp located at M44 has been proposed to functionally replace Asp at L213 in proton transfers (Hansen *et al.*, 1992a; Rongey *et al.*, 1993).

Evidence for the involvement of Ser-L223 in proton transfer comes from the drastic reduction of $k_{AB}^{(2)}$ (~10^2–10^3-fold) upon replacement of Ser-L223 with Ala or Asn and the restoration upon replacement with Thr or Asp (Paddock *et al.*, 1990a; Okamura & Feher, 1992). Takahashi and Wraight (1992) proposed a direct transfer of a proton from Asp-L213 to reduced Q_B and ascribed the drastic effects of the Ser-L223

to Ala replacement to structural changes. However, structural changes seem unlikely since the charge recombination rates k_{AD} and k_{BD}, the forward electron transfer rate k_{AB}[(1)], and the EPR spectrum of Q_B^- were all essentially the same in the mutant as in native RCs. More recently, Takahashi and Wraight (1993) proposed a model that is essentially the same as that proposed in this work (Paddock *et al.*, 1990a).

Additional support for the involvement of Ser-L223 in proton transfer comes from work in *Rhodopseudomonas viridis*, where a $\sim 10^3$-fold decrease in k_{AB}[(2)] was observed in a Ser → Ala mutant (Leibl *et al.*, 1993). Furthermore, X-ray crystallography shows no significant structural change beyond the amino acid replacements (Sinning *et al.*, 1990; Leibl *et al.*, 1993). Replacement of Ser-L223 with Ala inhibits growth in *Rb. capsulatus* (Bylina *et al.*, 1989, 1992), illustrating the importance of Ser-L223 in this system as well. These results strongly support the proposal that Ser-L223 is a component of a proton transfer chain.

The second proton transfer to reduced Q_B [H^+(2) in eq 6 and Figure 8] involves Glu-L212 (Paddock *et al.*, 1989; Takahashi & Wraight, 1992). The proton is transferred to Glu-L212 *via* proton donor group(s), possibly through a cluster of water molecules near the methoxy groups of Q_B (Beroza *et al.*, 1992). The closest proton donor residue, Asp-L213, is $\sim$7 Å away. Interestingly, replacement of Asp-L213 with Asn reduces the observed rate of proton uptake following single reduction of the quinones (McPherson *et al.*, 1991), suggesting that Asp-L213 is likely to also be important for proton transfer to Glu-L212. Proton transfer from Glu-L212 to the doubly reduced Q_B ($\sim$5 Å in the *Rb. sphaeroides* crystal structure; Allen *et al.*, 1988) may occur in several possible ways (Okamura & Feher, 1992): (1) directly if reduced Q_B can move, (2) indirectly through an intervening water molecule, or (3) indirectly through His-L190, which forms a hydrogen bond to Q_B. There is no evidence to support (3) since replacement of His-L190 with Gln retains a fast (within 5-fold of native values) steady-state cytochrome photooxidation rate (Williams *et al.*, unpublished results). To distinguish between possibilities (1) and (2), higher resolution X-ray data that resolve individual water molecules would be of great help. In addition, the X-ray structure of RCs with Q_B reduced would provide evidence for or against possibility (1).

ACKNOWLEDGMENT

We thank Ed Abresch for purification of the RCs.

APPENDIX: TITRATION OF TWO STRONGLY INTERACTING SITES

The electrostatic interaction between nearby residues can give rise to complicated titration behavior [for an excellent discussion see Edsall and Wyman (1958)]. Consider two acid residues HA_1 and HA_2 with pK_a[8] values of pK_a(1) and pK_a(2) for the isolated residues. The interaction between these residues raises the energy of the doubly ionized state $A_1^-A_2^-$ by an energy of ΔpK_a^{inter} (1 pK_a unit = 60 meV). The fractional protonation of the acid groups f_H(A1) and f_H(A2) can be calculated using the partition function for two residues [*e.g.*, see Bashford and Karplus (1991)]:

$$f_H(A1) = [1 + 10^{pH - pK_a(2)}]/Z \quad (A1)$$

$$f_H(A2) = [1 + 10^{pH - pK_a(1)}]/Z \quad (A2)$$

$$Z = 1 + 10^{pH - pK_a(1)} + 10^{pH - pK_a(2)} + 10^{2pH - pK_a(1) - pK_a(2) - \Delta pK_a^{inter}} \quad (A3)$$

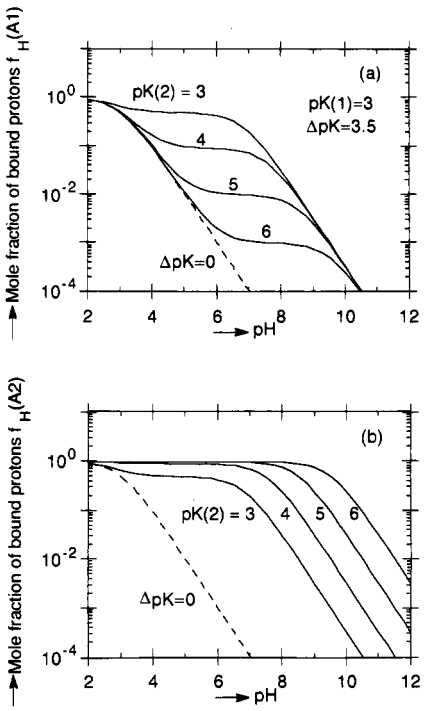

FIGURE 9: Calculated titration behavior for two coupled acids (solid lines) with $pK_a(2) \geq pK_a(1)$ interacting with an energy ΔpK_a^{inter}. For comparison, the titration behavior with no interaction (*i.e.*, $\Delta pK_a^{inter} = 0$) is shown (dashed lines). The mole fraction of bound protons f_H(A1) for HA_1 (a) and f_H(A2) for HA_2 (b) as a function of pH is shown with $pK_a(1) = 3$, $\Delta pK_a^{inter} = 3.5$, and $pK_a(2) = 3$, 4, 5 or 6 (see eqs A1–A3). The acid with the lower intrinsic pK_a (HA_1) partially titrates at pH = $pK_a(1)$, is relatively pH-independent for $pK_a(2) \leq pH \leq pK_a(2) + \Delta pK_a^{inter}$, and partially titrates above pH = $pK_a(2) + \Delta pK_a^{inter}$. The acid with the higher intrinsic pK_a (HA_2) titrates predominantly at pH $\geq pK_a(2) + \Delta pK_a^{inter}$.

The titration behavior of two interacting residues with $pK_a(1) = 3$, $\Delta pK_a^{inter} = 3.5$, and different values of $pK_a(2)$ (from 3 to 6) is shown in Figure 9. The titration of HA_1, the residue with the lower pK_a, is shown in Figure 9a. For comparison, the titration of the group in an isolated system (dashed line for $\Delta pK_a^{inter} = 0$, Figure 9a) shows a simple titration curve with a single break at pH 3. In the coupled system the fractional protonation also decreases near pH = $pK_a(1) = 3$. However it becomes relatively pH-independent at higher pH [Figure 9a; $pK_a(2) = 3$, 4, 5, and 6] as the second residue HA_2 starts to titrate, retarding the titration of HA_1 due to electrostatic repulsion between the two ionized acids. The fraction protonated finally decreases at pH above $pK_a(2) + \Delta pK_a^{inter}$ (pH = 6.5, 7.5, 8.5, and 9.5 in Figure 9a) as the dianionic state $A_1^-A_2^-$ is formed. In the pH-independent region, from $pK_a(1)$ to $pK_a(2) + \Delta pK_a^{inter}$, the ratio of HA_1 to HA_2 is determined by the difference in the pK_a values of the two acids: $HA_1/HA_2 = 10^{pK_a(1) - pK_a(2)}$ (Figure 9a).

The titration of HA_2, the residue with the higher intrinsic pK_a, is shown in Figure 9b. This residue remains mostly protonated until the pH = $pK_a(2) + \Delta pK_a^{inter}$ [*e.g.*, at pH = 9.5 for $pK_a(2) = 6$]. Thus the observed pK_a for the group with the higher pK_a is increased relative to the intrinsic pK_a by the interaction energy ΔpK_a^{inter}. [For a more detailed discussion of interacting groups see, *e.g.*, Yang *et al.* (1993)]. An interesting case occurs when the pK_a values of the two groups are nearly comparable [*e.g.*, $pK_a(1) = pK_a(2) = 3$]. In this case the two acid groups are significantly ionized in the intermediate pH region between $pK_a(1)$ and $pK_a(2) + \Delta pK_a^{inter}$ due to sharing of the proton between

roughly equivalent interacting acids. This can explain the titration behavior of Glu-L212. For example, if Glu-L212 interacts with a residue with a slightly lower pK_a, then some limited titration of Glu-L212 would occur below pH = pK_a + ΔpK_a^{inter}, where ΔpK_a^{inter} is the interaction between the two sites, and full titration would occur above that pH (see Figure 9b). This is consistent both with kinetic data, which suggest that Glu-L212 titrates mainly above pH 9.5 (Paddock *et al.*, 1989), and with infrared spectroscopy, which indicates that Glu-L212 is significantly ionized at pH ~ 7 (Hienerwadel *et al.*, 1992).

REFERENCES

Allen, J. P., Feher, G., Yeates, T. O., Komiya, H., & Rees, D. C. (1988) *Proc. Natl. Acad. Sci. U.S.A. 85*, 8487–8491.

Bashford, D., & Karplus, M. (1991) *J. Phys. Chem. 95*, 9556–9561.

Beroza, P., Fredkin, D., Okamura, M. Y., & Feher, G. (1992) in *The Photosynthetic Reaction Center II* (Breton, J., & Vermeglio, A., Eds.) pp 363–374, Plenum Press, New York.

Breton, J., & Vermeglio, A., Eds. (1988) *The Photosynthetic Bacterial Reaction Center, Structure and Dynamics*, Plenum Press, New York.

Breton, J., Thibodeau, D. L., Berthomieu, C., Mäntele, W., Vermeglio, A., & Nabedryk, E. (1991a) *FEBS Lett. 278*, 257–260.

Breton, J., Berthomieu, C., Thibodeau, D. L., & Nabedryk, E. (1991b) *FEBS Lett. 288*, 109–113.

Bylina, E. J., & Wong, R. (1992) in *Research in Photosynthesis* (Murata, N., Ed.) Vol. I, pp 369–372, Kluwer Academic Publishers, Dordrecht, The Netherlands.

Bylina, E. J., Jovine, R. V. M., & Youvan, D. C. (1989) *Bio/Technology 7*, 69–74.

Edsall, J. T., & Wyman, J. (1958) *Biophysical Chemistry*, p 699, Academic Press, New York.

Feher, G., Allen, J. P., Okamura, M. Y., & Rees, D. C. (1989) *Nature 339*, 111–116.

Feher, G., Paddock, M. L., Rongey, S. H., & Okamura, M. Y. (1992) in *Membrane Proteins: Structure, Interactions and Models* (Pullman *et al.*, Eds.) pp 481–495, Kluwer, Boston.

Gutman, M., & Nachliel, E. (1990) *Biochim. Biophys. Acta 1015*, 391–414.

Hansen, D. K., Nance, S. L., & Schiffer, M. (1992a) *Photosynth. Res. 32*, 147–153.

Hansen, D. K., Baciou, L., Tiede, D. M., Nance, S. L., Schiffer, M., & Sebban, P. (1992b) *Biochim. Biophys. Acta 1102*, 260–265.

Hegemann, P., Oesterhelt, D., & Steiner, M. (1985) *EMBO J. 4*, 2347–2350.

Hienerwadel, R., Thibodeau, D., Lenz, F., Nabedryk, E., Breton, J., Kreutz, W., & Mäntele, W. (1992) *Biochemistry 31*, 5799–5808.

Hienerwadel, R., Nabedryk, E., Paddock, M. L., Rongey, S. H., Okamura, M. Y., Mäntele, W., & Breton, J. (1993) in *Research in Photosynthesis* (Murata, N., Ed.) Vol. 1, pp 437–440, Kluwer Academic Publishers, Dordrecht, The Netherlands.

Kleinfeld, D., Okamura, M. Y., & Feher, G. (1984) *Biochim. Biophys. Acta 766*, 126–140.

Kleinfeld, D., Okamura, M. Y., & Feher, G. (1985) *Biochim. Biophys. Acta 809*, 291–310.

Labahn, A., Paddock, M. L., McPherson, P. H., Okamura, M. Y., & Feher, G. (1994) *J. Phys. Chem.* (in press).

Lanyi, J. K. (1986) *Biochemistry 25*, 6706–6711.

Leibl, W., Sinning, I., Ewald, G., Michel, H., & Breton, J. (1993) *Biochemistry 32*, 1958–1964.

Maróti, P., & Wraight, C. A. (1988) *Biochim. Biophys. Acta 934*, 329–347.

Maróti, P., & Wraight, C. A. (1990) in *Current Research in Photosynthesis* (Baltscheffsky, M., Ed.) Vol. 1, pp 1.165–1.168, Kluwer, Boston.

McPherson, P. H., Okamura, M. Y., & Feher, G. (1988) *Biochim. Biophys. Acta 934*, 348–368.

McPherson, P. H., Schonfeld, M., Paddock, M. L., Feher, G., & Okamura, M. Y. (1990) *Biophys. J. 57*, 404 (abstr.).

McPherson, P. H., Rongey, S. H., Paddock, M. L., Feher, G., & Okamura, M. Y. (1991) *Biophys. J. 59*, 142 (abstr.).

McPherson, P. H., Okamura, M. Y., & Feher, G. (1993a) *Biochim. Biophys. Acta 1144*, 309–324.

McPherson, P. H., Schonfeld, M., Paddock, M. L., Okamura, M. Y., & Feher, G. (1993b) *Biochemistry* (in press).

Nagle, J. F., & Tristram-Nagle, S. (1983) *J. Membr. Biol. 74*, 1–14.

Nakamaye, K. L., & Eckstein, F. (1986) *Nucleic Acids Res. 24*, 9679–9698.

Okamura, M. Y., & Feher, G. (1992) *Annu. Rev. Biochem. 61*, 861–896.

Okamura, M. Y., Paddock, M. L., McPherson, P. H., Rongey, S. H., & Feher, G. (1992) in *Research in Photosynthesis* (Murata, N., Ed.) Vol. 1, pp 349–356, Kluwer Academic Publishers, Dordrecht, The Netherlands.

Paddock, M. L., Rongey, S. H., Abresch, E. C., Feher, G., & Okamura, M. Y. (1988) *Photosynth. Res. 17*, 75–96.

Paddock, M. L., Rongey, S. H., Feher, G., & Okamura, M. Y. (1989) *Proc. Natl. Acad. Sci. U.S.A. 86*, 6602–6606.

Paddock, M. L., McPherson, P. H., Feher, G., & Okamura, M. Y. (1990a) *Proc. Natl. Acad. Sci. U.S.A. 87*, 6803–6807.

Paddock, M. L., Feher, G., & Okamura, M. Y. (1990b) *Biophys. J. 57*, 569 (abstr.).

Paddock, M. L., Rongey, S. H., McPherson, P. H., Feher, G., & Okamura, M. Y. (1991a) *Biophys. J. 59*, 142 (abstr.).

Paddock, M. L., Feher, G., & Okamura, M. Y. (1991b) *Photosynth. Res. 27*, 109–119.

Rongey, S. H., Paddock, M. L., McPherson, P. H., Feher, G., & Okamura, M. Y. (1991) *Biophys. J. 59*, 142 (abstr.).

Rongey, S. H., Paddock, M. L., Feher, G., & Okamura, M. Y. (1993) *Proc. Natl. Acad. Sci. U.S.A. 90*, 1325–1329.

Schulten, Z., & Schulten, K. (1986) *Methods Enzymol. 127*, 419–438.

Shinkarev, V., Takahashi, E., & Wraight, C. (1992) in *The Photosynthetic Reaction Center II* (Breton, J., & Vermeglio, A., Eds.) pp 375–387, Plenum Press, New York.

Simon, R., Proefer, U., & Puhler, A. (1983) *Bio/Technology 1*, 784–791.

Sinning, I., Koepke, J., Schiller, B., & Michel, H. (1990) *Z. Naturforsch. 45c*, 455–458.

Stewart, R. (1985) *The Proton: Applications to Organic Chemistry*, Academic Press, New York.

Subramaniam, S., Marti, T., & Khorana, H. G. (1990) *Proc. Natl. Acad. Sci. U.S.A. 87*, 1013–1017.

Takahashi, E., & Wraight, C. A. (1990) *Biochim. Biophys. Acta 1020*, 107–111.

Takahashi, E., & Wraight, C. A. (1991) *FEBS Lett. 283*, 140–144.

Takahashi, E., & Wraight, C. A. (1992) *Biochemistry 31*, 855–866.

Takahashi, E., & Wraight, C. A. (1993) in *Advances in Molecular and Cell Biology* (Barber, J., Ed.) JAI Press, Greenwich, CT (in press).

Tittor, J., Soell, C., Oesterhelt, D., & Steiner, M. (1989) *EMBO J. 8*, 3477–3482.

Van Gelder, B. F., & Slater, E. C. (1962) *Biochim. Biophys. Acta 58*, 593–595.

Warshel, A. (1986) *Methods Enzymol. 127*, 578–587.

Williams, J. C., Steiner, L. A., Feher, G., & Simon, M. I. (1984) *Proc. Natl. Acad. Sci. U.S.A. 81*, 7303–7307.

Yang, A.-S., Gunner, M. R., Sampogna, R., Sharp, K., & Honig, B. (1993) *Proteins: Struct., Funct., Genet. 15*, 252–265.